Supporting Information for "Linking Ocean Forcing and Atmospheric Interactions to Atlantic Multidecadal Variability in MPI-ESM1.2."

J. Oelsmann[1,3], L.Borchert[1,2,6], R.Hand[1,4,5], J.Baehr[2], J.Jungclaus[1]

[1]Max Planck Institute for Meteorology, Hamburg, Germany

[2]Institute for Oceanography, Center for Earth System Research and Sustainability (CEN), Universität Hamburg, Germany

[3]Deutsches Geodätisches Forschungsinstitut der Technischen Universität München, Germany

[4]Geographical Institute, University of Bern

[5]Oeschger Centre for Climate Research, University of Bern

[6]Sorbonne Universités (SU/CNRS/IRD/MNHN), LOCEAN Laboratory, Institut Pierre Simon Laplace (IPSL), Paris, France

Contents of this file

1. Supplementary Materials

   (i) AMV and surface heat flux responses

   (ii) AMV-pattern of SSTs, surface wind and sea level pressure

2. Figures S1 to S4

————

March 31, 2020, 4:14pm

AMV-conditions in heat-flux, restoring, control and slab-ocean simulations

We give additional insights in AMV-related responses for observations and the experiments which were not shown in the main article. For the control-simulation (hereinafter CONTROL) we show AMV-relationships referring to annual anomalies as well as to low-pass (11 year running-mean) filtered anomalies (all de-trended). In this way we follow the ideas of Gulev, Latif, Keenlyside, Park, and Koltermann (2013), who interpreted this separation as the short-term and the long-term, primarily ocean-driven variability. We are aware that lead-lag relationships derived from low-pass-filtered data can as well just reflect the filtered signal of stochastic atmospheric noise (Cane et al., 2017). Nevertheless, with the conclusions drawn from our idealised experiments, we have a strong argument that ocean dynamics are capable to drive similar responses as seen in the low-frequency regime (Gulev et al., 2013).

We interpret the ensemble-mean responses in the forced experiments (CPL-TH-REST and CPL-HEAT-FLUX) as the long-term responses associated with AMOC and AMV changes, due of the imposed multidecadal timescale of AMOC-oscillations. Comparison of these idealised experiments with the CONTROL run further helps to understand different AMV-relationships, when considering filtered or annual anomalies. In the following sections we demonstrate that the described mechanisms causing AMV in the idealised experiments, namely the ocean-driven subpolar NA heat release and the atmospheric sea level pressure response and sub/-tropical feedbacks, are also present in the CONTROL set-up.

AMV and surface heat flux responses

Figure S1 gives an overview of the total net surface heat flux (SHF) anomalies, either correlated with AMV or with AMOC26N. Among all coupled forced, or 'free' (CONTROL) simulations, we find good agreement concerning subpolar North Atlantic (NA) heat release on multidecadal timescales. This response occurs under both strong AMV or AMOC26N conditions and is caused by the multidecadal ocean heat convergence in the subpolar gyre (SPG) region, a key message of the main text. The similarity of the SHF-pattern in the CONTROL run at low-frequencies (Figures S4h and S4k) further supports validity of this mechanism in an unperturbed simulation.

The plots of the CPL-HEAT-FLUX experiment (Figures S4a and S4d) show, that much of the heat-flux signal, we identify as the response to AMOC/AMV variations, coincides with the applied NAO-forcing itself (shown in Figure S4). We therefore find much higher heat release in the Labrador Sea (LS) region than in CPL-TH-REST, because heat extraction by the external forcing is still active at lag 0. Hence, we argue that we cannot investigate, without reserve, atmospheric responses to those heat-flux anomalies in CPL-HEAT-FLUX as they are potentially biased by the forcing.

The similar SHF responses in the CONTROL or CPL-TH-REST simulation suggest similar atmospheric responses on multidecadal timescales. Thus, we investigate whether the proposed atmospheric mechanisms, which amplify the tropical AMV-branch, also exist in the CONTROL simulation.

AMV-pattern of SSTs, surface wind and sea level pressure

We analyze regression maps of AMV-SLP-responses at the annual and the multidecadal timescale by applying 11 year running-means to the data from observations, CONTROL and SLAB-OM in Figure S2. We use observed SSTs from HadISST 1.1 (Rayner, 2003) and SLP data from 20CRv2 (Compo et al., 2011) in the time period between 1900-2012. In Figures S2e and S2f we also illustrate differences in the SLP-responses when taking the 5-member ensemble mean of the CPL-TH-REST experiment, or when appending the runs successively.

On the annual timescale, we find an approximately dipolar SLP-pattern in observations, CONTROL and CPL-TH-REST at lag 0 (Figures S2a,c and e). According to Clement et al. (2015) this is the short-term signature of atmospheric forcing and was associated with the NAO (here a negative phase). This pattern very well reflects the annual AMV-related SLP anomalies found in SLAB-OM (Figure S2g), or those shown in Clement et al. (2015), respectively.

The multidecadal responses in Figures S2b,d and f, derived by either filtering (observations, CONTROL) or averaging the ensemble (CPL-TH-REST), indicate a large low-SLP response covering the Central North and Tropical Atlantic. Because these large scale SLP-response over the NA overall coincide, we expect similar atmospheric mechanisms to cause the tropical AMV-SST response. The slab-ocean model (Figure S2h) is no capable in reproducing this observed multidecadal atmospheric feature of AMV. We show that the low-frequency SLP response in observations is more consistent with those anomalies generated by distinct long-term AMOC fluctuations in Figure S2f.

The SST, SLP and wind regression maps further indicate similar atmospheric circulation anomalies during a positive AMV in CONTROL and the other coupled sensitivity experiments on long timescales (Figures S3a, b, d). All patterns are regressed onto AMV at lag 0 and, as in the previous examples, we separate the annual from the multidecadal timescale in CONTROL.

In agreement Clement et al. (2015), the short-term SST, SLP and wind response in the slab-ocean experiment in Figure S3f matches well the response in the equivalent coupled CONTROL (Figure S3e) simulation, which are derived from unfilered annual anomalies. Here, atmospheric conditions are characterized by reversed trade-winds, the dipolar SLP-pattern, midlatitude easterly anomalies and the tripolar SST response. Still the N-E-Atlantic high pressure anomaly in CONTROL (Figure S3f) is more pronounced than in SLAB-OM, which mostly resembles barotropic NAO conditions.

The multidecadal SST, SLP and wind responses in CONTROL (filtered, Figure S3d) share several characteristics with the AMV-responses in the coupled experiments (Figures S3a and S3b). We find an enhanced low SLP anomaly east of the maximum SST anomalies in the SPG-region. These low SLP-anomalies reach southwards to the tropics, where similar south-westerly surface wind anomalies occur (Figures S3a, b, d). Hence, we argue that the same mechanisms, the WES feedback effect and anomalous lower tropospheric heat transport discovered in CPL-TH-REST, also cause the tropical SST-limb in the CONTROL simulation. This assertion is supported by the positive tropical SHF anomalies found on multidecadal timescales in CONTROL (Figure S1).

Because we find much stronger AMV-related SST anomalies in the coupled, forced experiments, which is due to the strong induced AMOC phases, we hypothesize that the atmospheric responses in Figures S3a and S3b show more distinct low SLP anomalies in the Central Atlantic and downstream of the heat-source compared to the CONTROL experiment. Overall, the similar multidecadal atmospheric AMV-conditions in observations, CONTROL and CPL-TH-REST consolidate the low-frequency atmospheric responses and associated feed-back mechanisms identified by analysis of the idealised experiments.

References

Cane, M. A., Clement, A. C., Murphy, L. N., & Bellomo, K. (2017). Low-Pass Filtering, Heat Flux, and Atlantic Multidecadal Variability. *Journal of Climate*, *30*(18), 7529–7553. doi: 10.1175/JCLI-D-16-0810.1

Clement, A., Bellomo, K., Murphy, L. N., Cane, M. A., Mauritsen, T., Rädel, G., & Stevens, B. (2015). The Atlantic Multidecadal Oscillation without a role for ocean circulation. *Science (New York, N.Y.)*, *350*(6258), 320–324. doi: 10.1126/science.aab3980

Compo, G. P., Whitaker, J. S., Sardeshmukh, P. D., Matsui, N., Allan, R. J., Yin, X., . . . Worley, S. J. (2011). The twentieth century reanalysis project. *Quarterly Journal of the Royal Meteorological Society*, *137*(654), 1-28. Retrieved from `https://rmets.onlinelibrary.wiley.com/doi/abs/10.1002/qj.776` doi: 10.1002/qj.776

Gulev, S. K., Latif, M., Keenlyside, N., Park, W., & Koltermann, K. P. (2013). North Atlantic Ocean control on surface heat flux on multidecadal timescales. *Nature*, *499*(7459), 464–467. doi: 10.1038/nature12268

Rayner, N. A. (2003). Global analyses of sea surface temperature, sea ice, and night marine air temperature since the late nineteenth century. *Journal of Geophysical Research*, *108*(D14), 14. doi: 10.1029/2002JD002670
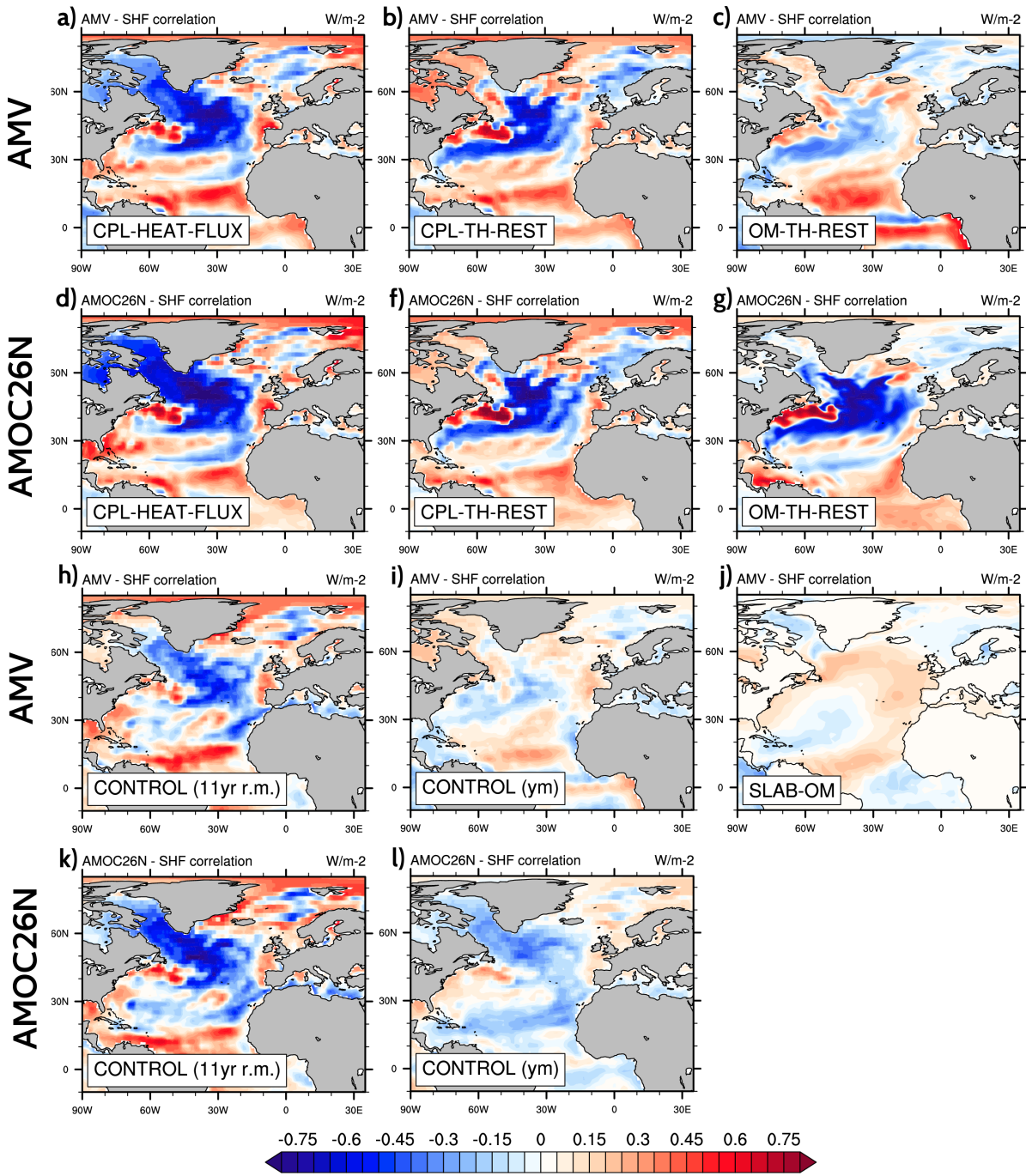
Figure S1. Point-wise correlations of annual total surface heat flux anomalies with AMV and AMOC26N at lag 0 for all experiments. We additionally show correlation maps based on 11 year running-mean filtered anomalies for CONTROL (h,k). Negative values denote fluxes out of the ocean and vice versa.
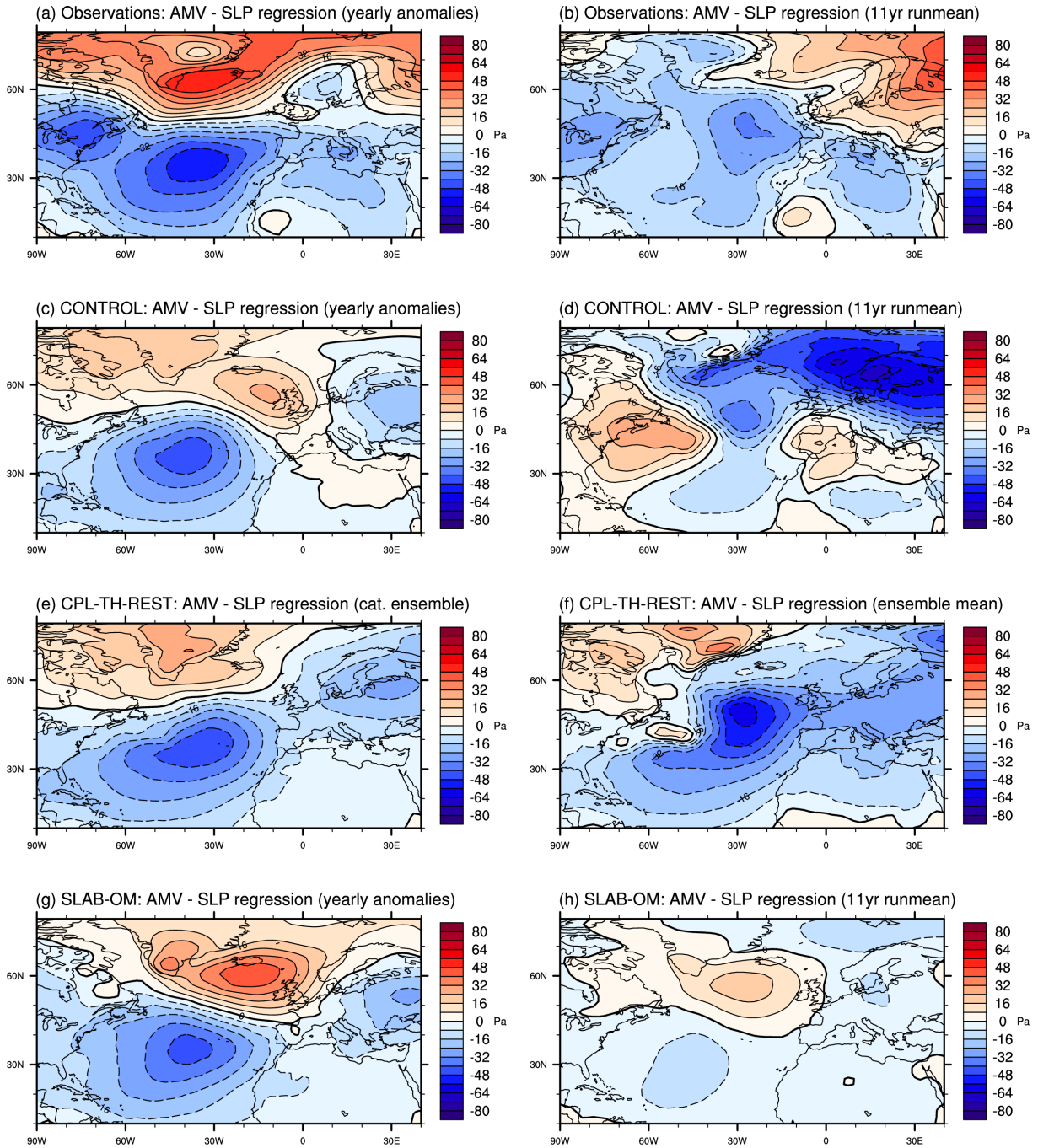
March 31, 2020, 4:14pm

Figure S2. SLP anomalies associated with a change of one-standard-deviation AMV. Regression-pattern are computed for annual and 11-year-lowpass-filtered det-trended AMV anomalies for Observations (a,b), CONTROL (c,d), and SLAB-OM (g,h). For CPL-TH-REST we show the responses when all runs are successively concatenated (e) and for the ensemble mean (f), respectively.
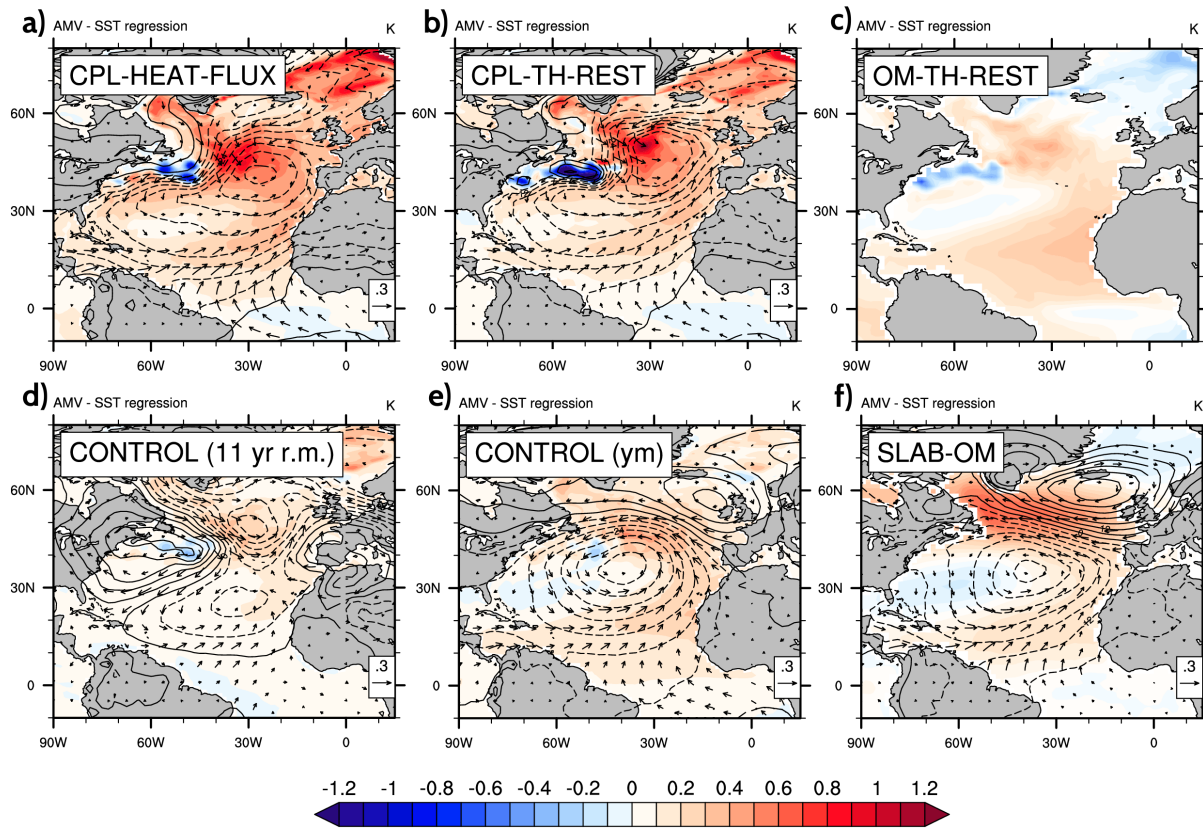
Figure S3. Annual SSTs (shading, K), SLP (dashed contours for negative anomalies, 6hPa intervals) and 10m wind anomalies (m/s) associated with a change of one-standard-deviation AMV at lag0 for all experiments. For the CONTROL run we show regressions of annual anomalies (e) and 11 year running-means (d).
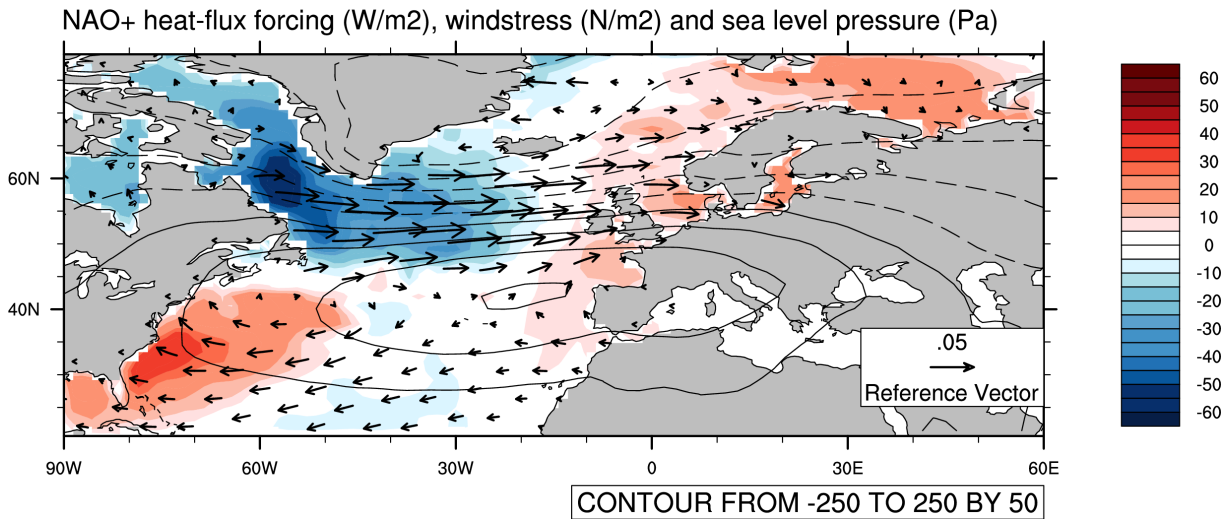
NAO+ heat-flux forcing (W/m2), windstress (N/m2) and sea level pressure (Pa)

Figure S4. Spatial pattern of the surface heat-flux forcing (shading, negative out of the ocean) for CPL-HEAT-FLUX in W/m2. Additionally, SLP (contours in Pa, negative dashed) and wind stress (N/m2) anomalies (averaged over DJFM) associated with a positive two-standard-deviation change of the NAO are given. Note that no anomalous wind stress forcing is implemented.

March 31, 2020, 4:14pm